

# INVESTIGATION OF COUPLER BREAKDOWN THRESHOLDS FOR PLASMA PROCESSING OF FRIB QUARTER-WAVE RESONATORS WITH FUNDAMENTAL AND HIGHER-ORDER MODES\*

P. Tutt<sup>†</sup>, W. Hartung, S. H. Kim, T. Xu

Facility for Rare Isotope Beams, Michigan State University, East Lansing, MI, USA

## Abstract

FRIB is developing plasma processing techniques for in-situ recovery of cavity performance in linac cryomodules during long-term user operation. While plasma processing has been shown to be effective for high-frequency (0.8 - 1.5 GHz) elliptical cavities, one of the challenges for FRIB is to avoid plasma breakdown in the fundamental input coupler (FPC), which has relatively weak coupling strength ( $Q_{ext}$  ranging from  $2E6$  to  $1E7$ ). FRIB cavities are not equipped with higher-order-mode (HOM) couplers; however, in preliminary tests, we found that HOMs are suitable for plasma processing of FRIB Quarter-Wave Resonators (QWRs) driven via the FPC. In this study, we investigated plasma breakdown thresholds in the fundamental and the first 2 HOMs for the FRIB  $\beta = 0.085$  QWRs. Electric field distributions in the FPC region and cavity region were calculated for the room-temperature case using CST Microwave Studio's frequency domain solver (FDS). Simulation results will be presented, with a comparison of breakdown thresholds inferred from the RF modeling to the experimental results.

## INTRODUCTION

The Facility for Rare Isotope Beams is an accelerator facility that supports a heavy ion linac for nuclear physics research. The linac consists of both quarter-wave resonators (QWR) and half-way resonators (HWR) in its 46 cryomodules. In order to maintain the linac for long-term user operation, mitigation of degrading effects like multipacting and field emission in the superconducting cavities is essential. Plasma processing has been identified as a good technique to reduce field emission at the Spallation Neutron Source (SNS), Fermilab, and others. [1-3]. The technique is advantageous to other surface treatments for Niobium like electropolishing and high-temperature baking because it can be deployed in-situ with the cryomodule.

While plasma processing has been demonstrated to be successful in a wide variety of cavity geometries, there are challenges posed by the potential ignition of the fundamental power coupler (FPC). If ignition occurs within the FPC, the FPC could be damaged or copper from the antenna may be sputtered onto the Niobium surface. Avoidance of this ignition is critical for the implementation of this technique for in-situ use with the cryomodule. In the case of the FRIB

$\beta = 0.085$  QWR, the value of  $Q_{ext}$  is on the order of  $10^6$  to  $10^7$  which is much greater than the room temperature  $Q_0$ . To improve the coupling of the FPC to the cavity, higher-order modes (HOM) have been investigated as potential candidates for processing which have improved coupling at room temperature.

To investigate the breakdown thresholds for the cavity and coupler volumes of the FRIB  $\beta = 0.085$  QWR, CST Microwave Studio (MWS) was used to simulate the electric field distribution inside the cavity and FPC for the fundamental and first two HOMs [4]. Experimental measurements are used to infer the electric field at ignition from the CST model. A theoretical model for the breakdown was adapted from JLab to describe  $\beta = 0.085$  QWR for comparison.

## CST MWS SIMULATION

To understand the electric field distribution inside the cavity and coupler volumes, CST MWS was used to simulate field distributions at plasma processing conditions. An eigenmode solver was used to assess the cavity fields, but a frequency-driven solver is needed to accurately assess the coupler fields. A mismatch results from room temperature conditions, which were simulated by the inclusion of material with room temperature conductivity of Niobium surrounding the CST model.

A large mismatch between  $Q_0$  and  $Q_{ext}$  at the fundamental mode implies that the power delivery to the cavity is poor and reflection is high in the FPC. Not only does this make ignition in the cavity difficult, but a high reflection coefficient can create a standing wave with high electric fields in the FPC that could cause breakdown. HOMs improve the mismatch and have been shown to be effective at FRIB in QWRs and at Fermilab. [5, 6]. Using FDS, the S-parameters were used to identify the first three resonant frequencies which are shown in Table 1. Field distributions were calculated at the resonant frequencies.

Table 1: Resonant Frequencies

Mode	Frequency [MHz]
TEM $\lambda/4$	80.120
TEM $3\lambda/4$	240.92
TEM $5\lambda/4$	402.24

## Characterizing E-field for Breakdown

In determining the threshold electric field, several considerations must be made for how breakdown is occurring

\* Work supported by the U.S. Department of Energy, Office of Science, Office of Nuclear Physics and used resources of the Facility for Rare Isotope Beams (FRIB) under Award Number DE-SC0000661.

<sup>†</sup> tutt@frib.msu.edu

Content from this work may be used under the terms of the CC BY 4.0 licence (© 2023). Any distribution of this work must maintain attribution to the author(s), title of the work, publisher, and DOI

within the cavity and FPC volumes. First, the electric field was analyzed in two ways corresponding to different ideas about how ionization is occurring. One approach was to find the peak surface electric field in the cavity and FPC.  $E_p$  in the FPC was found along the inner conductor of the transmission line as shown in Fig. 1 for each mode in Table 1.  $E_p$  in the cavity was found along the bottom of the inner conductor as shown in Fig. 2 for each mode in Table 1. In an ideal QWR case at HOMs, the additional regions of a high electric field in HOMs should be the same as the peak field at the bottom of the inner conductor; however, for the practical case, the local maximum above the bottom of the inner conductor has a smaller  $E_p$ . The coupler tip field was neglected when considering electric fields within the FPC. This was done since the tip of the coupler is inside the cavity volume in the cryomodule setup, so it cannot cause breakdown inside the FPC. This approach of using the peak surface field assumes that during the ionization process, the electron is always experiencing the field of  $E_p$ .

Another approach is to consider how the fields vary in space and consider that the electron may not always experience  $E_p$ . This idea considers several different electron paths that have the highest voltage. The voltage was obtained by integrating the electric field on the direction of travel. Dividing the voltage by the path length gives a spatially averaged electric field  $E_{avg}$ . This quantity was calculated for several path lengths including the inner conductor nose to the tuning plate, accelerating gap, and pickup port to the inner conductor. A similar idea is applied to the FPC, where the integration of the electric field begins where the peak surface field in the FPC is found.

### Simulation Results

The highest value of  $E_{avg}$  was found below the accelerating gap between the inner conductor and the beam port. The path length is the shortest of all paths considered. Figure 3 shows  $E_{avg}$  for the cavity and FPC volumes for the first three modes. Cavity fields were normalized to the stored energy in the cavity at ignition. This information was inferred from measurements of forward and reflected power. The forward power for ignition of the FPC and cavity are shown in Fig. 4. FPC fields were normalized to the forward power at ignition. As seen in Fig. 3, cavity ignition fields occur at a lower average electric field whereas coupler ignition fields occur at higher electric fields. It should be noted while the use of HOMs improves coupling at room temperature, the required RF power for ignition increases with frequency, which may present challenges for the use of even higher frequency modes and cavities of different geometries.

## THEORETICAL MODEL

For comparison to the simulated fields, a model for microwave breakdown was developed based on gas parameters and the geometry of the cavity and FPC. Following the frequency-dependent model developed by JLab for a 5-cell elliptical cavity, electron loss through ionization may be de-

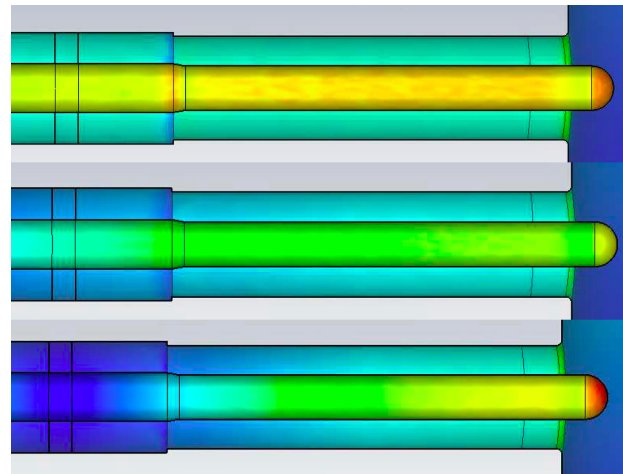


Figure 1: FPC field distributions. From top to bottom: Fundamental mode, first HOM, second HOM.

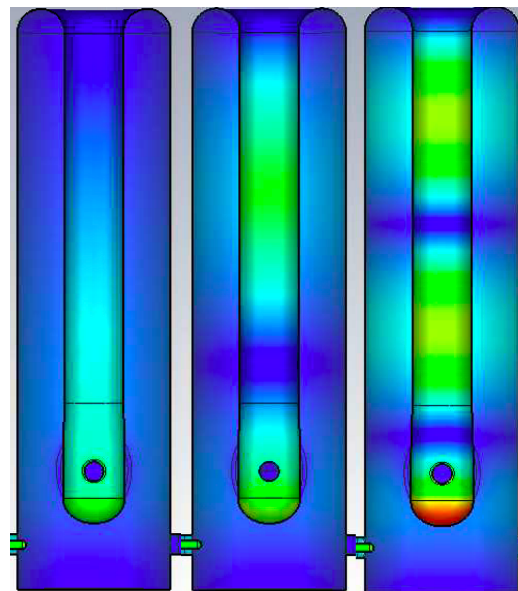


Figure 2: Cavity field distributions. From left to right: Fundamental mode, first HOM, second HOM.

scribed by mechanisms of diffusion loss and attachment [7,8]. Similar assumptions are made about the negligibility of the attachment rate and that all power goes towards ionization. The breakdown criteria can therefore be written as a function of the geometry of the cavity or FPC, gas parameters, and the driving frequency. Equation (1) defines this relationship

$$E_i^2 = \frac{\ell^2}{\Lambda^2} \frac{mu_i}{3e} (v_m^2 + \omega^2) \quad (1)$$

where  $\ell$  is the mean free path,  $\Lambda$  is the effective diffusion length,  $m$  is the mass of the electron,  $u_i$  is the ionization potential,  $e$  is the elementary charge,  $v_m$  is the electron-neutral collision frequency, and  $\omega$  is the operating frequency. Unlike the derivation given by Jlab,  $v_m^2 \ll \omega^2$  is not assumed to be true because the operating frequency is in the MHz range rather than the GHz range like for JLab's elliptical cav-

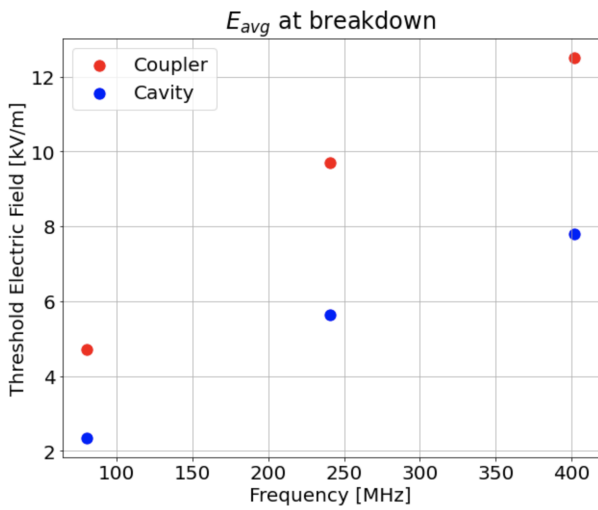


Figure 3: Measured ignition thresholds inferred from simulation for FPC and cavity volumes.

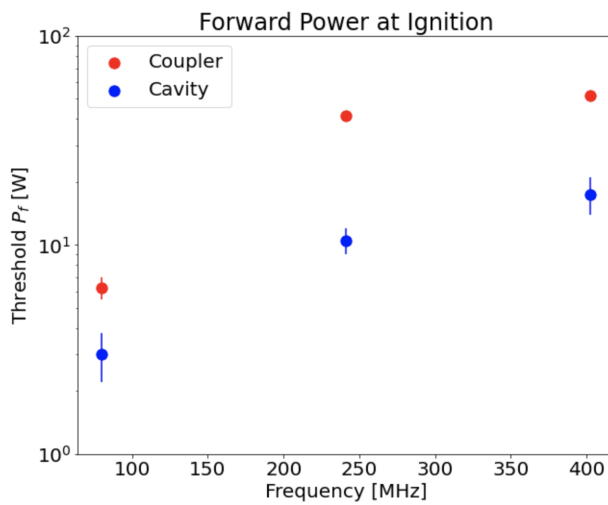


Figure 4: Forward power at ignition for FPC and cavity.

ities. Values for ionization potential, mean free path length, and electron-neutral collision frequency were determined using literature with a pressure of 100 mTorr and with a gas species of Neon. While the real gas mixture contains 95% Neon and 5% Oxygen, we ignore the contributions of oxygen to simplify the model. Gas parameters and other relevant experimental parameters are shown in Table 2. [9].

Table 2: Gas Parameters

Parameter	Value	Symbol
Mean Free Path	1.2 cm	$\ell$
$e^-$ Collision Frequency	$1.2 * 10^8$ Hz	$\nu_m$
Ionization Potential	21.4 eV	IP
Gas Species	Neon	Ne
Pressure	100 mTorr	p

## Determining Effective Diffusion Length

While parameters like  $u_i$ ,  $\nu_m$ , and  $\ell$  are based on gas species and pressure,  $\Lambda$  is determined by the geometry of the volume. The effective diffusion length for electrons describes how far they must travel to reach the wall of the container.  $\Lambda$  must be determined for the geometry of the FPC and the cavity. The FPC is a simple coaxial line, while the cavity geometry is more complicated. The QWR resembles a coaxial structure but is shorted at one and open at the other end such that the inner conductor does not connect from end to end. Literature provides ways to calculate the diffusion length for simple geometries such as a cylinder, sphere, or parallel plates [7]. With some adaptations to the cylinder case, a description can be found for a coaxial line where  $\Lambda$  is a function of the inner and outer conductor radius. For the FPC, this description is sufficient.

Calculations of  $\Lambda$  for the FPC were done using the coaxial line and parallel plate description where each wall is the inner and outer conductor. Each method yielded a similar value for  $\Lambda$  of 3.17 mm. The cavity geometry is more complex but since it still reflects a coaxial structure, the coaxial approach was taken to calculate  $\Lambda$ . Two sets of dimensions were used in the calculation. One reflects the nominal dimensions of the QWR as a cylinder while the other reflects the dimensions around the accelerating gap. The two cases yield  $\Lambda$  values of 26.7 mm and 18.3 mm respectively to each case. Both of these  $\Lambda$  values will be used to draw theoretical breakdown curves.

## RESULTS

With a theoretical description for breakdown determined for the cavity and FPC, the simulated electric fields inferred from the experiment may be compared to the model. Figure 5 plots the cavity breakdown field with theoretical curves and simulated fields at ignition. Two curves are drawn for the theoretical breakdown corresponding to two different values of  $\Lambda$ . The highest spatially averaged field around the accelerating gap is plotted in red. In addition, the peak surface electric field along the spatially averaged field is included. The inclusion of this quantity will be discussed in the next section. Figure 6 contains a similar plot for the FPC.

## DISCUSSION

To analyze the results presented, the limitations of the theoretical model must be addressed. The theory utilized assumes the simplest case of high-frequency breakdown where ionization is counteracted by loss of electrons due to diffusion. An important limitation of diffusion theory is the mean free path limit. If the dimensions of a container become comparable to the electron mean free path for that container, diffusion theory can no longer be applied as collisions with the wall of the container cannot be neglected [10]. For a gas species of Neon and a pressure of 100 mTorr, the mean free path is 12 mm as shown in Table 2. For the cavity



Content from this work may be used under the terms of the CC BY 4.0 licence (© 2023). Any distribution of this work must maintain attribution to the author(s), title of the work, publisher, and DOI

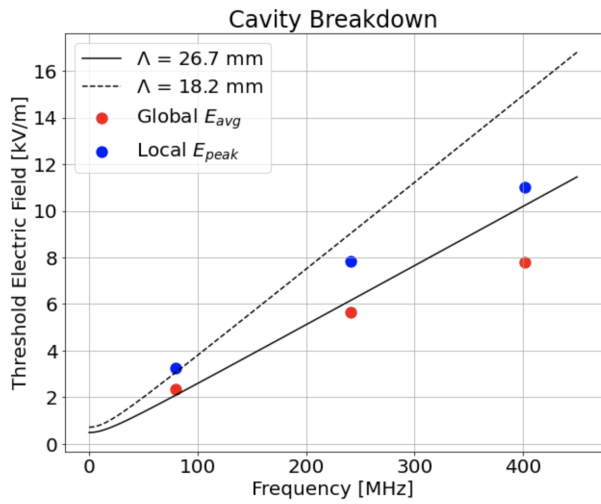


Figure 5: Spatially averaged electric field and peak surface electric field around accelerating gap.

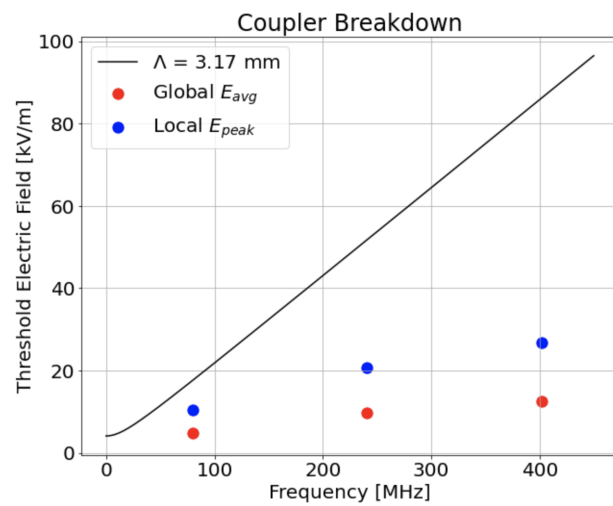


Figure 6: Spatially averaged electric field and peak surface electric field in FPC.

case, lambda is calculated to be 26.7 mm or 18.2 mm depending on the geometries considered; however, the lambda value for the FPC is only 3.17 mm with a separation between inner and outer conductors of 10 mm. This indicates that the theoretical model used is a sufficient description for the cavity, but not for the coupler. A different description would be required to model the FPC volume where other processes than diffusion become important. For example, electrons may collide with the wall of the FPC. This effect is negligible for the cavity volume but not for the FPC. This mean free path limitation is demonstrated in Fig. 3, where the fit between theory and measured fields inferred from the simulation is very poor. In addition to a mean free path limit, there is a uniform field limit for diffusion theory which relates the pressure of the system, the wavelength of the applied field, and the effective diffusion length [10]. For both the FPC and cavity at each applied field, the uniform

field limit is not violated; however, this limit is formulated from the field between parallel plates. More work is needed to translate this description to coaxial like geometries.

As discussed above, the mean free path limit is not exceeded for the cavity so the theoretical model should apply. Figure 5 shows two sets of field values calculated for each mode. Upon the initial investigation of the electric field distributions, the peak surface electric field was considered as discussed earlier. This idea corresponds to how breakdown would occur where the highest possible field is. When these values were originally compared to theory, they were much higher than the  $\Lambda = 26.7$  mm prediction. This motivated the use of a spatially averaged electric field. The highest spatially averaged field was found around the accelerating gap between the beam port and the inner conductor where the path length is very small and the field is high. These quantities are plotted in red. Plotted in blue is the peak surface field along the spatially averaged path which occurs on the inner conductor. The motivation for using this quantity is that  $E_{avg}$  doesn't appear to fit the theoretical predictions well beyond the fundamental mode. The use of  $E_{avg}$  was because it provides a spatially averaged field between two different walls of the cavity that describes how an electron may not feel  $E_p$  during the entire ionization process. While this accounts for how the electron may experience different fields in space, the expectation is still that breakdown will first occur in the area with the highest fields. The area with the highest  $E_{avg}$  could therefore be used to identify regions where breakdown would occur first; however, the peak surface field along the path that  $E_{avg}$  is calculated would still be the field at which the electron experiences breakdown. These peak surface fields at the location of spatial averaging along the inner conductor provide a better fit to the theoretical model.

While the fit is improved with the use of  $E_p$  at the point of highest spatial averaging around the accelerating gap, there is still a wide variation between the two theoretical models especially at high frequency. This makes the comparison between measurement and theory somewhat difficult. Neither theoretical model appears to match the behavior of the inferred fields at a high frequency well, which could mean that our model is not a good description of the QWR in reality. A more rigorous approach to the calculation of  $\Lambda$  may be needed utilizing numerical integration techniques. Since the model for the FPC is not valid given the previously discussed mean free path limit, additional phenomena must be considered to account for the observed breakdown at much lower fields. Collisions with the walls of the FPC will be more frequent compared to the cavity and neglected terms in the breakdown description such as attachment rate may play an important role.

## SUMMARY

CST MWS was used to simulate electromagnetic field distributions in the FRIB  $\beta = 0.085$  QWR and FPC at plasma processing conditions. A theoretical model was developed

for high-frequency microwave breakdown based on gas parameters and volume geometry. The goal of this study was to understand the breakdown field within the FPC due to the dangerous effects associated with FPC ignition during plasma processing. Due to the mean free path limit of the diffusion theory-based model, the FPC breakdown could not be predicted. The cavity breakdown is not constrained by the mean free path limit and with the appropriate selection of the peak surface field at the location of the highest spatially averaged electric field, the measured breakdown inferred from simulation lies between the theoretical prediction for two different effective diffusion lengths calculated for the cavity.

### Future Work

Future work will be oriented toward developing an appropriate breakdown model for the FPC. A more rigorous treatment of the effective diffusion length in the cavity is also needed so that an electric field value, whether it be global  $E_p$ , a local  $E_p$ , or  $E_{avg}$ , may be confirmed as the parameter controlling the breakdown within the cavity. Simulation work will be extended to other geometries of FRIB cavities that are being processed such as the  $\beta = 0.53$  HWR. Other plasma limitations like the oscillation amplitude limit of Neon need to be investigated for both the FPC and cavity volumes. Ideas like the uniform field limit which is based on simple geometries like parallel plates must be extended to describe coaxial geometries so that the FPC and cavity volume can be confirmed as not violating this limit.

### ACKNOWLEDGMENTS

Initial work on this study was supported by the MSU Accelerator Science and Engineering Traineeship program.

Useful discussions with the SRF plasma processing teams at Fermilab, ICJLab, and Argonne National Lab were beneficial for this project.

### REFERENCES

- [1] M. Doleans *et al.*, “Plasma Processing R&D for the SNS Superconducting Linac RF Cavities”, in *Proc. SRF’13*, Paris, France, Sep. 2013, paper TUP057, pp. 551–557.
- [2] S.-H. Kim *et al.*, “Overview of ten-year operation of the superconducting linear accelerator at the Spallation Neutron Source”, *Nucl. Instrum. Methods Phys. Res., Sect. A*, vol. 852, p. 20–32, Apr. 2017. doi:10.1016/j.nima.2017.02.009
- [3] P. Berrutti, *et al.*, “Plasma ignition and detection for in-situ cleaning of 1.3 GHz 9-cell cavities”, *J. Appl. Phys.*, vol. 126, p. 023302, 2019. doi:10.1063/1.5092235
- [4] CST Studio Suite, “CST Microwave Studio”, 2023. <http://www.cst.com>
- [5] W. Hartung *et al.*, “Investigation of Plasma Processing for Coaxial Resonators”, presented at SRF’23, Grand Rapids, MI, USA, Jun. 2023, paper THIXA01, this conference.
- [6] P. Berrutti, “Plasma Cleaning R&D at FNAL”, presented at the Jun. 2018 TeSLA Technology Collaboration Meeting, Saitama, Japan.
- [7] S. C. Brown, *Introduction to Electrical Discharges in Gases*, Wiley, New York, 1966.
- [8] S. Popovic *et al.*, “Resonant-frequency discharge in a multi-cell radio frequency cavity”, *J. Appl. Phys.*, vol. 116, p. 173301, 2014. doi:10.1063/1.4900994
- [9] Yu. P. Raizer, *Gas Discharge Physics*, Springer-Verlag, Berlin, 1991.
- [10] S. C. Brown and A. D. MacDonald, “Limits for the Diffusion Theory of High Frequency Gas Discharge Breakdown”, *Phys. Rev.*, vol. 76, pp. 1629-1633, 1949. doi:10.1103/PhysRev.76.1629